The Seebeck Coefficient of BiCuOSe:Ca and a Comparison of the Carrier Concentration of ITO and BiCuOSe:Ca through Hall and Chaikin and Beni Anaylsis

By Rachel Waite
Oregon State University
Department of Physics
2011

ABSTRACT:

The Seebeck coefficient of a material is the voltage produced by that material when a temperature gradient has been introduced between its two ends. The Seebeck coefficient is important because it tells us the sign of the carriers present and can be used to help in energy conservation as heat is transformed into a potential. In this report the Seebeck coefficient of p-type BiCuOeSe:Ca semiconductors on MgO substrates were determined experimentally between temperatures of 60-300 K using the a method in which a small temperature gradient (about 4 K) is applied to two ends of the sample and is measured by a differential thermocouple while the potential created by the sample is also measured. Doping levels varied from 1.79% to 2.38%. Subsequent measurements are taken as both the temperature gradient and the potential of the sample return to 0. At low temperatures BiCuOSe:Ca behaved metallically, that is the Seebeck coefficient decreased linearly with temperature. The Seebeck coefficient did not decrease with increased doping as expected and in fact the amount of doping had no relation to the Seebeck coefficients of the samples, but the amount of doping was similar among the samples and thus no real conclusion could be drawn between the amount of doping of the BiCuOSe:Ca samples and their Seebeck coefficient.

At the high temperature limit of 300 K the carrier concentration was determined through Hall analysis and also through the method by Chaikin and Beni in which the carrier concentration depends only on the Seebeck coefficient. The method was tested on previous indium tin oxide (ITO) data and then on BiCuOSe:Ca. Both types of samples indicate a large disagreement (by at least an order of magnitude) between the two theoretical carrier concentrations (with the method by Chaikin and Beni being higher than that of the Hall theory). It is believed that this large difference is due in part to not enough neighboring interactions being taken into account (with the Chaikin and Beni method) and also that 300 K may not be a high enough temperature limit to apply the model. It was determined that a high temperature limit is between 2000-10,000 K by solving for the temperature at which both models would be in agreement.

Table Of Contents

Section 1: Introduction

The purpose of this paper is to experimentally determine the Seebeck coefficient of BiCuOSe:Ca as the temperature of the sample decreases, and to determine how various levels of doping BiCuOSe with calcium affect the Seebeck at these different temperatures. This paper also investigates how the carrier concentration changes with temperature. The carrier concentration can be determined by knowing the resistivity, the Seebeck coefficient, and the lattice parameters of the material. BiCuOSe has lattice parameters a=b= 3.921 Å, c = 8.913 Å (Stampler, et al. 2008) (Zakutayev, et al. 2011).). It is arranged in "alternating layers of $[Cu_2Se_2]^{2-}$ tetrahedra and anti-flourite $[Bi_2O_2]^{2+}$ distorted tetrahedra in a tetragonal P4/nmm structure" (Tate, et al. 2008) (P4/nmm refers to the space group of the material). Fig. 1.1 shows the lattice structure of BiCuOSe.

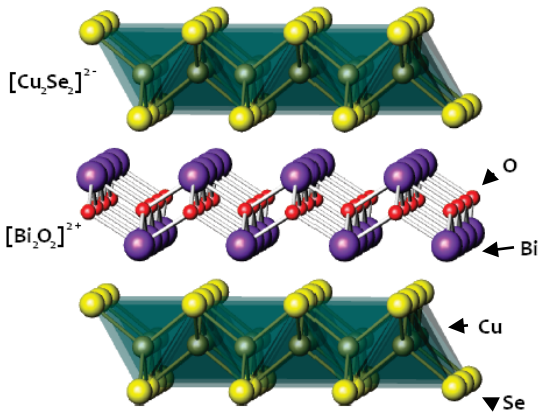

Figure 1.1: *The BiCuOSe atomic structure. This picture was taken from* (Stampler, et al. 2008). *The red dots represent oxygen, the purple represent bismuth, the gold represent copper, and the yellow represent selenium.*

The Seebeck effect, named after Thomas Johann Seebeck who discovered it in the early 1820's, is the ability of a material to produce a voltage when a temperature gradient is introduced between its two ends (Seebeck 1822). It is the basis for thermocouple physics. He found that when two different metals are joined together and their junctions are held at different temperatures, a current flows between them (Fig. 1.2).

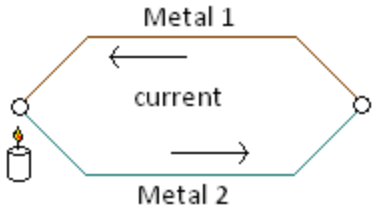

Figure 1.2: *T.J Seebeck found that current will flow between two different metals if their junctions are held at different temperatures.*

Here the Seebeck effect of different BiCuOSe (bismuth copper oxy selenide) thin films doped with varying levels of calcium on MgO (magnesium oxide), and $SrTiO_3$ (strontium titanate) substrates were measured at varying temperatures. (Doping is the term given to creating impurities in the crystal lattice structure of the material).

Electrons can only exist in certain energy levels in an atom. When two or more atoms combine to form a molecule their atomic energy levels also combine. The combination of energy levels of molecules creates a continuum of energy levels called *bands.* The two main bands are the *valence band* and the *conduction band*. The valence band consists of the highest filled energy levels (Tan, et al. 1994). The conduction band consists of the higher energy levels of a material, it is responsible for electrical conduction because its energy levels are mostly empty electrons are free to move around whereas in the valence band there are not a lot of free states available for the electrons to move into (Singh 1994).

The density of states determines the allowed energy levels of a material and is given by:

$$D(E) = \frac{dW(k)}{dE} \qquad 1.1$$

where $W(k)$ is the volume of particle in k-space

$$W(k) = c_n k^n \quad 1.2$$

. ***K*** is a vector determined by the molecular wave equation in 3-space

$$|\psi_{\boldsymbol{k}} > = \frac{1}{\sqrt{N}} \sum_{\boldsymbol{R}} e^{\,i\boldsymbol{k}\cdot\boldsymbol{R}} |\boldsymbol{R}> \quad 1.3$$

where ***R*** is a lattice vector extending out from the origin of the lattice to any point in the lattice, *N* is the number of lattice sites, and ***k*** is the wave vector in 3-space given by:

$$\boldsymbol{k}_{x,y,z} = \frac{2\pi m}{Na} \quad 1.4$$

a is the lattice parameter (in either x, y, or z direction) and *m* is just an integer.

Plotting the energy vs. the density of states yields a graphical representation of valence and conduction bands (Fig. 1.3).

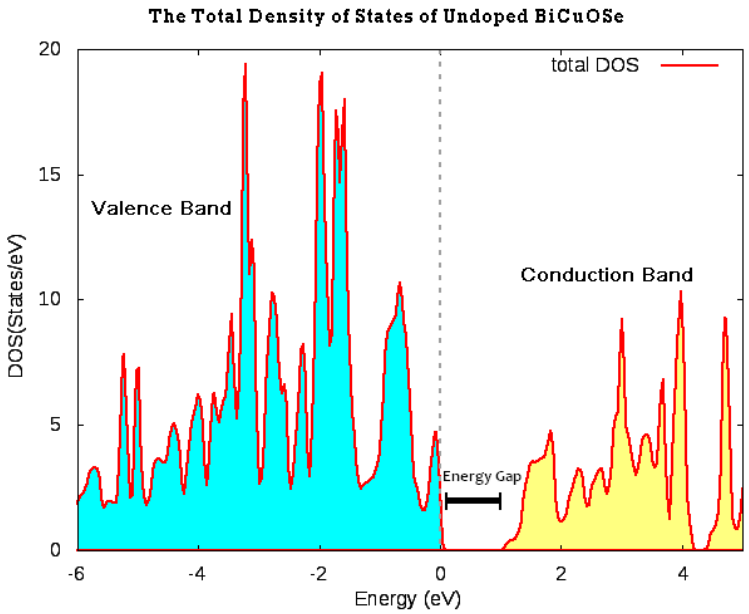

Figure 1.3: *The DOS plotted against energy gives a graphical representation of the valence and conduction bands. This is a plot of the DOS of undoped BiCuOSe using the Wein2K program with a k-mesh of 100 points. See Appendix B for lattice sites of BiCuOSe.*

In semiconductors and insulators there is a gap between the conduction and valence band, in metals the valence and conduction bands overlap. The Fermi energy (E_F) denotes the highest filled electron state at T = 0. The Fermi function *F(E)* tells us the probability of an electron having a certain energy

$$F(E) = \frac{1}{e^{(E-E_F)/(kT)}+1} \quad 1.5$$

where *E* is the energy level in question, E_F is the Fermi energy, *k* is the Boltzmann constant (8.617 * 10-5 eV/K, not to be confused with the vector, ***k***), and *T* is the temperature.

In metals, the conduction band and the valence band overlap and the Fermi level exists *in* the conduction band. This means that conduction can technically occur at any temperature. In semiconductors there is a bandgap between the valence and conduction band, but with enough applied energy an electron is able to jump from the valence band to the conduction band, enabling conductivity.

Doping introduces impurities into the crystal lattice of the semiconductor which can create new energy levels near the conduction or valence band. There are two different kinds of doping: *n*-type and *p*-type. *N*-type doping refers to the addition of energy levels in the band gap that are closer to the conduction band (raising the Fermi level). This means that it takes less energy to excite these electrons to the conduction band. This occurs when a semiconductor is doped with an atom with more than enough electrons to satisfy the bonds, leaving extra electrons to move through the semiconductor more easily. Atoms that are used to create an *n*-type semiconductor are called “donors” because they donate an extra electron. In n-type semiconductors the electrons are the *majority* carriers and the holes are the *minority* carriers. *P*-type doping creates energy levels near the valence band (effectively lowering the Fermi level) by atoms with not enough electrons to satisfy all of the bonds of the atom it replaces, in this way “holes” are introduced to the valence band . The electrons from neighboring atoms to try to complete the bond, leaving their atom a positively charged ion. Electrons move through the crystal by filling in the holes, making the holes themselves move from atom to atom. Atoms used to create *p*-type semiconductors are called “acceptors” because they readily accept neighboring electrons[2]. The holes are now the majority carriers and the electrons are the minority carriers. It is important to note that

doping leaves the semiconductor neutrally charged (that is, it does not change the charge of the molecule).

Undoped BiCuOSe consists of $[Cu_2Se_2]^{2+}$ and $[Bi_2O_2]^{2-}$ molecules connected together such that all of the bonds are satisfied (Tate, et al. 2008). BiCuOSe:Ca is a *p*-type semiconductor with holes in its valence band created by calcium. When BiCuOSe is doped with calcium, the calcium replaces a small fraction of the bismuth and only supplies two electrons for bonding, creating a hole in the valence band. In BiCuOSe, two atoms per unit cell are hosts to the carriers.

The way that the Seebeck effect happens is that one end of the material is heated while the other end is cold. This heat is a form of energy which excites the carriers. Carriers will diffuse from the hot end to the cold. In *p*-type semiconductors the holes move towards the cold side giving the cold side a positive potential with respect to the hot side, whereas in *n*-type semiconductors the free electrons move towards the cold side giving it a negative potential with respect to the hot side. The Seebeck coefficient is then calculated in microvolts per Kelvin as:

$$S = -\frac{(V_{Hot} - V_{Cold})}{T_{Hot} - T_{Cold}} \qquad 1.6$$

which gives the negative of the potential of the hot block with respect to the cold over the temperature gradient of the hot block with respect to the cold. This tells us that for *n*-type semiconductors the Seebeck coefficient will be negative while for *p*-type semiconductors the Seebeck coefficient will be positive (Kasap 1996) (Easley 2003). "The sign of the Seebeck coefficient represents the potential of the cold side with respect to the hot side." (Kasap 1996).

Previous Seebeck coefficient measurements indicate that undoped BiCuOSe has a Seebeck coefficient that *increases* with decreasing temperature while heavily doped BiCuOSe:Ca has a Seebeck coefficient that behaves metallically with decreasing temperature (Fig. 1.4) (Zakutayev, et al. 2011). An increasing Seebeck coefficient with decreasing temperature is due to phonon drag, which is the increase of the effective mass of the carriers. This paper will determine how minimal doping with Ca effects the Seebeck coefficient behavior with decreasing temperature.

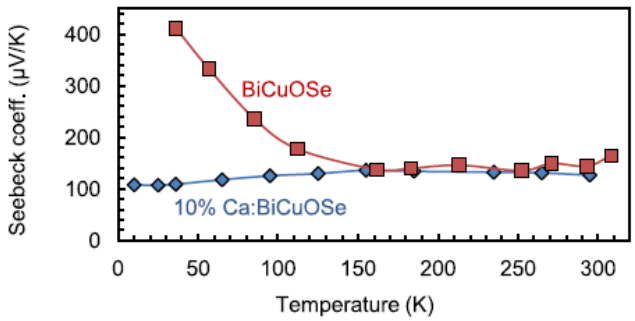

Figure 1.4: *Previous measurements of undoped BiCuOSe show a Seebeck coefficient trend that increases significantly with decreasing temperature due to phonon drag while BiCuOSe:Ca doped with 10% Ca shows a more metallic trend as the Seebeck coefficient decreases linearly with temperature. This data taken from* (Zakutayev, et al. 2011).

There is a method proposed by Chaikin and Beni (Chaikin and Beni 1976) (Easley 2003) in which the carrier concentration can be determined for a high temperature limit. They propose that in a high enough temperature limit the Seebeck coefficient can be determined solely by the carrier concentration, the Boltzmann constant, and the absolute value of the charge of an electron.

The Seebeck coefficient (which they refer to as "thermoelectric power") is:

$$S = -\frac{S^{(2)}/S^{(1)} + \mu/e}{T} \qquad 1.7$$

where $S^{(1)}$ and $S^{(2)}$ are determined from the Hamiltonian, the chemical potential, and energy and flux operators, μ is the chemical potential, T is the temperature, and e is the absolute value of the electron charge. However, in the high temperature limit, the Seebeck coefficient simplifies to one of the following (given certain restrictions):

	Region of Applicability	*Seebeck Coefficient*
Fermions With Spin	$kT \gg U_0, U_j$	$-\frac{k}{\lvert e\rvert}\ln\frac{2-c}{c}$
On-Site Repulsion	$U_0 \gg kT \gg U_j, T$	$-\frac{k}{\lvert e\rvert}\ln\frac{2(1-c)}{c}$
Nearest-Neighbor Interactions	$U_0 > U_1 > kT \gg U_{j>1}, T$	$-\frac{k}{\lvert e\rvert}\ln\frac{2(1-2c)^2}{c(1-c)}$
General Form	$U_0 > U_1 \ldots U_b > kT \gg U_{j>b}, T$	$-\frac{k}{\lvert e\rvert}\ln\frac{2(1-bc-c)^{b+1}}{c(1-bc)^b}$

k is the Boltzmann Constant, U_0 is the on-site coulomb interaction, U_j is the j^{th} neighbor interaction (b is an integer), and c is the ratio of particles to sites. The carrier concentration is

$$\rho_{CB} = \frac{c}{V} \quad 1.8$$

V is the volume of a lattice cell.

This paper compares the first three theories (fermions with spin, on-site repulsion, and nearest neighbor interactions) to the Hall theory of the carrier concentration.

The Hall theory gives the carrier concentrations as:

$$\rho_H = -\frac{B_z I_x}{dV_H e} \quad 1.9$$

where B_z is the applied magnetic field (in the z direction), I_x is the current (in the x direction), *d* is the film thickness, V_H is the measured Hall voltage, and *e* is the electron charge. (Hall carrier concentrations of ITO were determined by Prof. Brandon Brown, Department of Physics, University of San Francisco, and Hall carrier concentrations of BiCuOSe:Ca were determined by Jason Francis, Department of Physics (graduate student), Oregon State University).

First, these methods are compared to the carrier concentration and Seebeck coefficient data of ITO and then the method is used to compare with that of BiCuOSe:Ca.

There are two important assumptions made in analyzing the data of both materials. The first is that ITO only has eight carrier host sites per cell. The second is that 300 K is a high enough temperature limit. This paper also explores a theory for determining a high temperature limit.

ITO is an n-type semiconductor with a cubic lattice (in the Ia3 space group) of *a* = 10.117 Å (Gonzalez, et al. 2001) (Tahar, et al. 1998). It has 80 atoms per unit cell, it is uncertain just exactly how many atoms are carrier hosts, however the assumption that only eight contribute in ITO was taken from “Neutron diffraction study on the defect structure of indium-tin-oxide” by González, Cohen, Hwang, and Mason.

Section 2: Methods

The Seebeck coefficient of BiCuOSe:Ca thin-film semiconductors (on SrTiO3 (strontium titanate)) was measured relative to Cu (which has a Seebeck coefficient of about 2 μV/K at 300 K) (Kasap 1996) using a method in which one end of the sample is heated and the other is not. This creates a small temperature gradient between the two ends of the sample. A Seebeck voltage is then generated across the sample. This voltage is measured and the Seebeck coefficient is calculated from Equation 1.2. (Typical temperature gradients are between 1-5 K, in this lab the temperature gradients were between 3-5 K, and for most materials the voltages are in the range of millivolts, yielding a Seebeck coefficient between 10-100 μV/K). The base temperature of the entire system can be varied from 60-300 K with the use of a closed cycle refrigerator.

Experimental Setup:

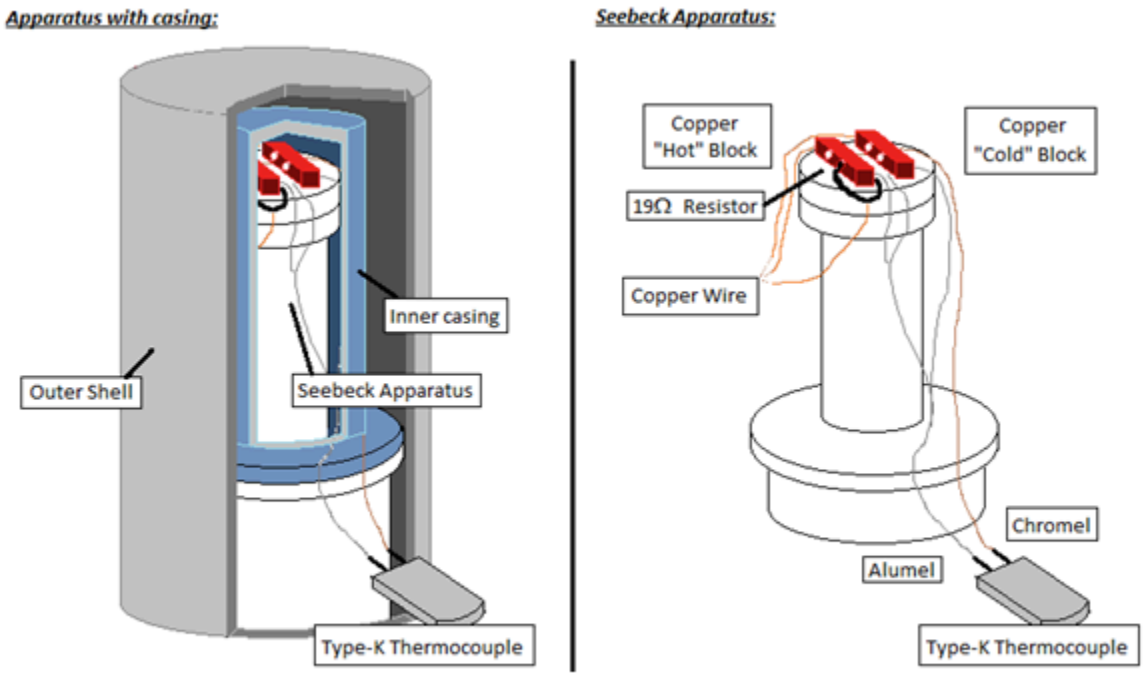

Figure 2.1: *The Seebeck Apparatus: the left diagram shows the Seebeck apparatus enclosed in a cryogenic vacuum casing used for temperature control while the right shows the Seebeck apparatus. A sample is placed between the hot and cold blocks which produces a voltage when the blocks are at different temperatures.*

The apparatus (Fig. 2. 1) consists of two copper blocks sitting on top of an insulated column; these blocks are in thermal contact with the column, but remain electrically isolated from it. A 19 □ resistor is placed in one of the copper blocks and is connected to a Keithley 2400 Source Meter. The meter is used to apply a voltage of 5 V to the 19 Ω resistor, effectively heating the block (this creates the 3-5 K temperature gradient between the blocks at room temperature). This block is referred to as the "hot" block. The resistor is insulated from the copper block such that no current flows between the "hot" block itself and the Source Meter.

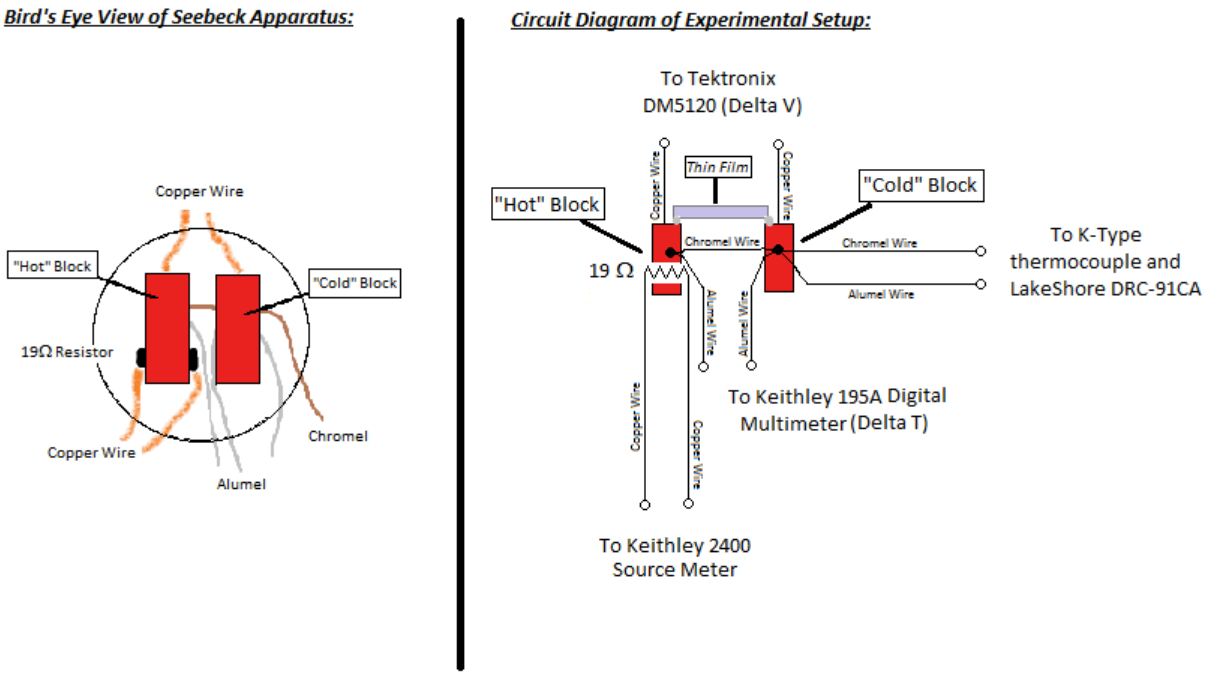

Figure 2.2: *The Seebeck Setup: the left diagram shows a bird's eye view of the Seebeck Apparatus and the right shows a circuit diagram of the experimental setup. The left block is heated using a 19 Ω resistor while the cold block is held at the temperature of the chamber. A thin film sample is placed between the blocks which produces a voltage read by the Tektronix DM5120 while the Keithley 195A Digital Multimeter measures the temperature gradient between the blocks. Plotting the potential difference over the temperature gradient gives us the Seebeck coefficient.*

A copper wire connects to the hot block and a copper wire connects to the cold block (Fig. 2.2), these wires go to the Tektronix DM5120 Programmable Digital Multimeter which records the potential difference between the two blocks produced by the sample once a temperature gradient has been introduced between them. Next, a type K thermocouple (Fig. 2.3) of chromel (a p-type metal consisting of 90% nickel 10% chromium) (MatWeb Material Property Data 1996) and alumel (an n-type metal consisting of 95% nickel, 2% manganese, 2% aluminum, and 1% silicon (MatWeb Material Property Data. 1996) wires is used to measure the temperature of the cold block (which is effectively the temperature

of the entire system) with respect to room temperature; the ends of the chromel and alumel wires are fused together to the cold block and the other ends are connected to the LakeShore DRC-91CA temperature controller which is pre-calibrated to convert the potential to Kelvins. A differential thermocouple (Fig. 2.4) of chromel fused at both ends with alumel connects to the hot and cold blocks respectively. The potential between the two open ends of the alumel wires is read by the Keithley 195A Digital multimeter; this potential is converted to Kelvins using Chart 2.1. A differential thermocouple is one in where two junctions are created between two dissimilar metals; one of the metals is severed such that a potential difference can be measured between the two severed ends corresponding to the potential difference between the junctions when the junctions are at different temperatures (OMEGA Engineering 2003) (Kasap 1996). A normal (in this case, a K-type) thermocouple utilizes one junction of two dissimilar metals (chromel and alumel) held at some temperature while the potential is measured between the two open ends held at some other temperature (in this case room temperature).

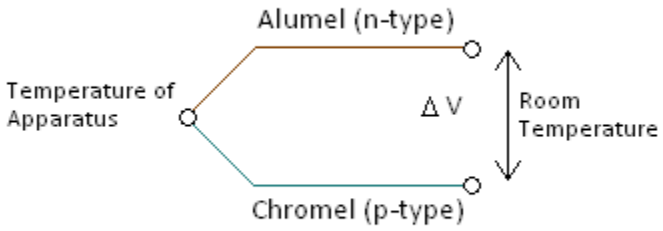

Figure 2.3: *The k-type thermocouple measures the potential difference between chromel and alumel created when two ends are fused together and held at the temperature of the Seebeck apparatus and the other two ends are held at room temperature. The potential gradient is measured between the two open ends at room temperature and is then converted to Kelvin by the Lakeshore Temperature Controller.*

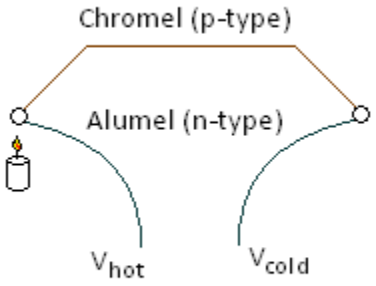

Figure 2.4: *The differential thermocouple measures the temperature gradient between the hot and cold blocks. One end of each alumel wire is fused together with a singe chromel wire and the junctions are connected to the hot block and the cold blocks respectively. The differential thermocouple measures the potential difference between the two open ends of the alumel wire and the potential is then converted to Kelvin using the Type-K Seebeck calibration chart (Chart 2.1).*

Procedure:

The surface of both copper blocks is sanded clean and wiped down with methanol, indium strips are laid down, and then the sample is clamped onto the indium strips via screws and a plastic clamp. These strips are used to establish a good electrical connection between the copper blocks and the sample; good electrical contact is essential to measuring the Seebeck coefficient so the two blocks must be as clean as possible. (Care must be taken not to make the connection too large as it decreases the resistance between the sample and the blocks which can result in a lower Seebeck coefficient). This resistance is measured by the multimeter before the Seebeck coefficient is measured and tells us how good the contacts between the sample and the blocks are.

At room temperature a potential of 5 V is applied by the Keithley 2400 Source Meter to the hot block's resistor, heating the block until the thermocouple connected to the Keithley 195A Digital multimeter reads a 0.15 mV potential gradient between the hot and cold blocks. The applied voltage is then returned to 0 V (that is, no more heat is applied to the hot block). Using the LabView computer program (Easley 2003) data is taken as the hot end of the sample cools back down to the temperature of the apparatus (and the potential gradients of the sample and of the thermocouple are returned to 0). LabView records the temperature of the apparatus (the Lakeshore DRC-91CA), the differential thermocouple voltage (the Keithley 195A), and the voltage produced by the sample (the Tekronix DM5120).

When taking temperature-dependent data the Seebeck apparatus is isolated in an inner casing and then enclosed in an outer shell which is clamped down at the base to ensure a proper seal of the cryochamber. The chamber is then vacuum sealed to about 2 * 10-6 Torr and the temperature is varied using a closed cycle helium refrigeration system. The helium is pumped into the chamber with a compressor, it immediately expands in the vacuum and cools the chamber to (in this experiment) 60 K. At sufficient pressure, the helium will push down a piston, allowing it to return to the compressor and repeat the process. A silicon diode situated at the base of the column in the Seebeck apparatus (not

shown in Fig. 2.1) applies heat to the system using the LakeShore 320 Autotuning Temperature Controller. When the temperature of the 320 Autotuning temperature controller is the same as that of the LakeShore DRC-91CA temperature controller the system is in thermal equilibrium and the Seebeck coefficient may be measured. At very low temperatures the potential gradient is a lot smaller, this is because at low temperatures the Seebeck calibration is much smaller and a small change in the potential corresponds to a large change in the temperature gradient.

Analyzing Data:

The data is then analyzed in an excel spreadsheet (Easley 2003). The differential thermocouple voltage must be converted to Kelvins using the conversion chart (Fig. 2. 4) which gives known Seebeck coefficient of the k-type thermocouple at varying temperatures (the Lakeshore Controller tells us the temperature of the apparatus and the chart gives the corresponding Seebeck coefficient of a chromel-alumel thermocouple at that temperature, so the potential read by the differential thermocouple connected to the Keithley 195A is divided by the Seebeck coefficient to convert the potential to Kelvins). Next the voltage produced by the sample is plotted against the temperature gradient and the slope of the line gives us the Seebeck coefficient of the sample in microvolts per Kelvin:

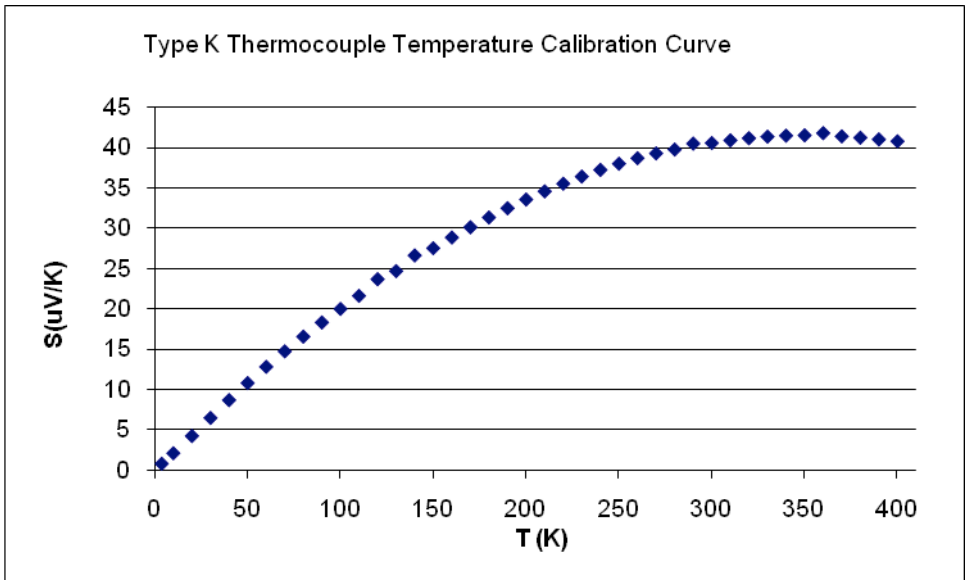

Figure 2.4*: The type K Seebeck coefficient thermocouple temperature calibration curve. Taken from: The calibration of thermocouples and thermocouple materials [microform] / G.W. Burns and M.G. Scroger. QC100 .U565 no.250-35.* Valley Library.

Section 3: Results

All four samples of BiCuOSe:Ca where first measured at room temperature and then again at subsequent intervals of 10 K from temperatures ranging from 60 K all the way up to 300 K (room temperature) while the chamber was approximately 2.8 * 10^{-6} Torr. Note that all Seebeck coefficient measurements are relative to Cu (which has a Seebeck coefficient of approximately 1.83 µV/K at room temperature). The resistance of the material relative to the copper blocks and indium strips was also measured as the temperature varied. This tells us how well of a connection the sample was making with the blocks during the measurement. This is important because at low temperatures the resistance tends to go down.

The samples of BiCuOSe:Ca were meant to be doped with 6% Ca meaning that 6% of the Bi was to be replaced with Ca, however, due to technical difficulties with the equipment, the samples were not doped at 6%. These samples were made with different degrees of *fluence* (the amount of energy used to create each sample). Sample 110222 (2.38% Ca) was made with a fluence of 1.5 J/m^2, sample 110223 (1.79% Ca) with 1.0 J/m^2, sample 110223-03 (2.37% Ca) with 1.75 J/m^2, and sample 110224 (2.27% Ca) with 1.25 J/m^2 (see Appendix C). Appendix C gives the Hall parameters measured by Jason Francis, Department of Physics (graduate student), Oregon State University, including the chemical composition of each sample.

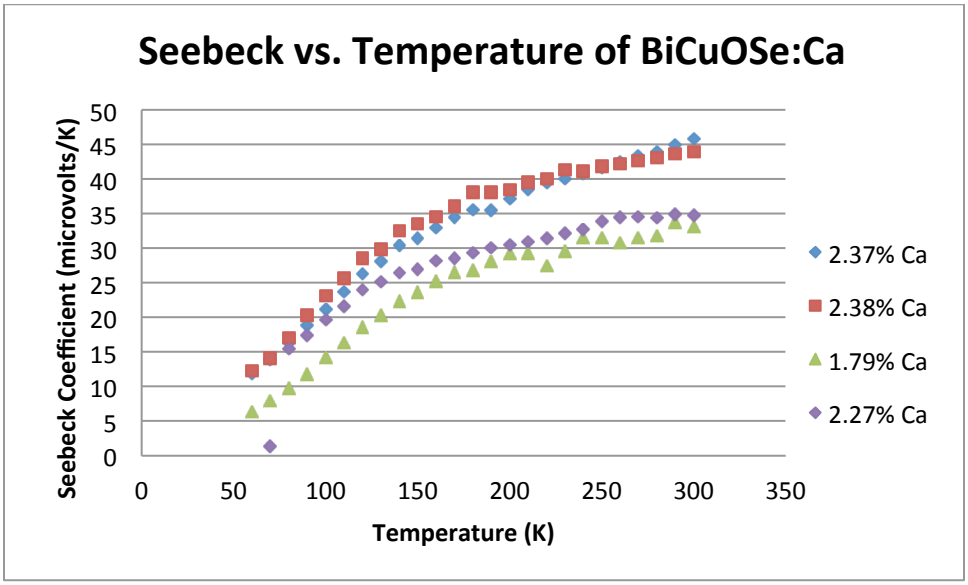

Figure 3.1: *This shows the Seebeck coefficient trends of the BiCuOSe:Ca samples measures as a function of temperature. Notice that they all to follow the same metallic trend, that is, they all to decline linearly with decreasing temperature.*

These samples seem to have a metallic trend, that is, their Seebeck coefficients decrease linearly with temperature (Fig. 3.1). This behavior is seen for all levels of doping and is consistent with the previous BiCuOSe:Ca trends as reported in Zakutayev, 2011. It is apparent that for BiCuOSe:Ca doped with as little as 1.79% Ca that the behavior of the material is metallic and does not exhibit phonon drag as does undoped BiCuOSe.

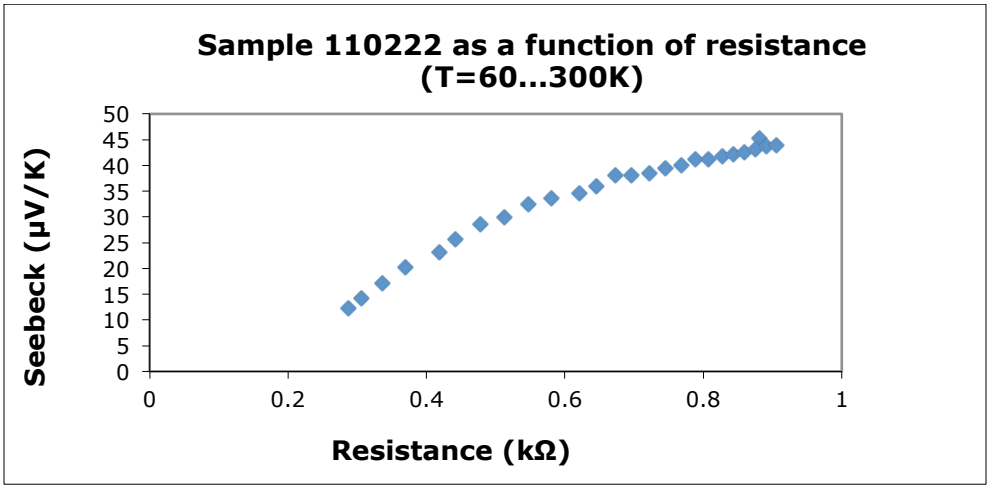

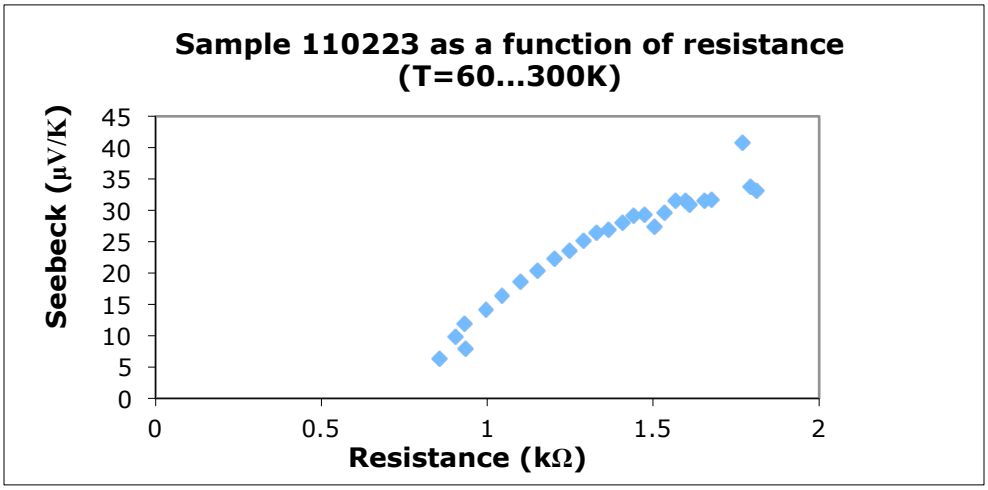

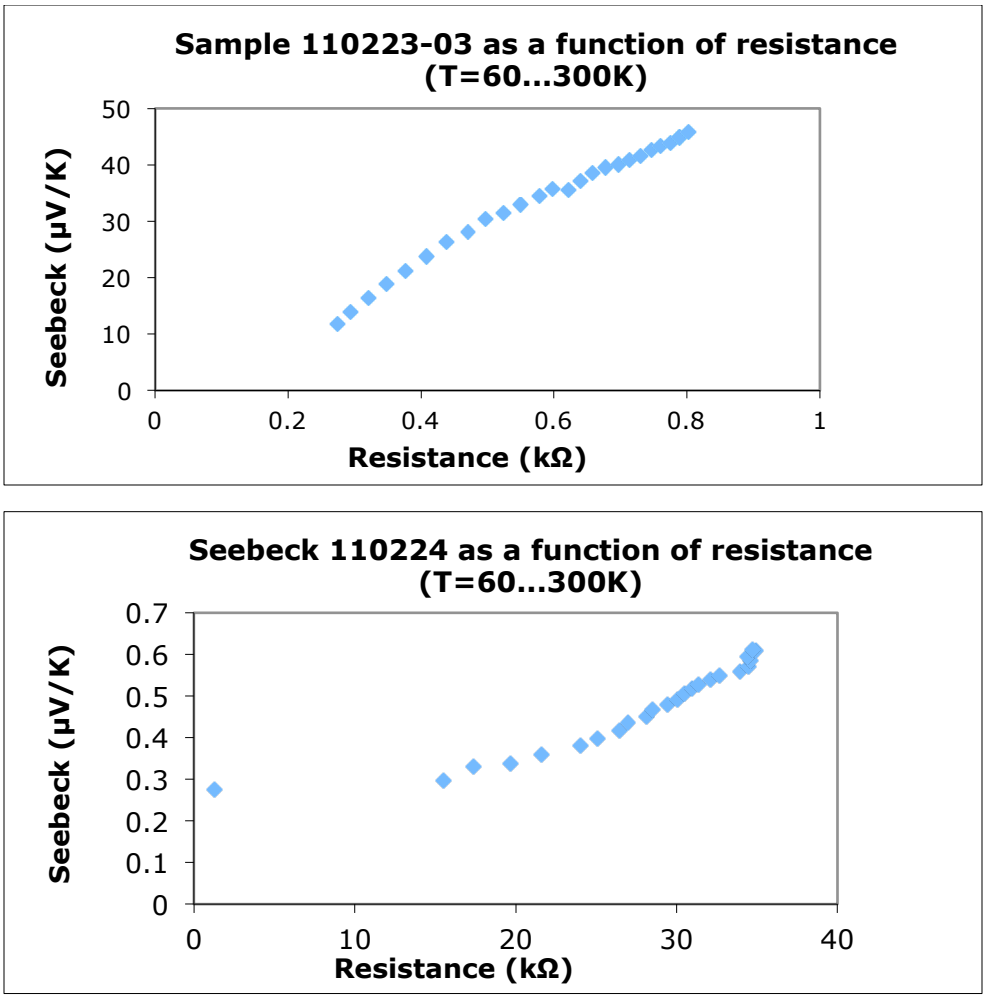

Figure 3.4: *Seebeck coefficients of the BiCuOSe:Ca samples as a function of resistance. Notice how Sample 110224 stands out from the rest.*

Sample 110223-03 has an almost linear relationship between the resistance and the Seebeck coefficient indicating that they are both changing at a constant rate with the temperature. Samples 110222 and 110223 have a resistance that increases more rapidly with temperature than does the Seebeck coefficient and Sample 110224 has the opposite trend; the Seebeck coefficient increases more rapidly with temperature than does the resistance. It is uncertain why this affect happens and unfortunately I was not able to duplicate the temperature dependent readings on these samples due to equipment malfunctions.

The contacts that the sample makes with the copper blocks is hard to duplicate exactly as the amount of indium in direct contact with the samples and the blocks was not the same from sample to sample nor even between one day to the next for a disturbed sample (that is, if the sample was physically removed

and then replaced). Thus, no real conclusion can be made about the resistance readings of the samples at varying temperatures.

It is not clear from all four temperature dependent readings whether the amount of Ca present in the sample bears any relation to the Seebeck coefficients obtained (the Seebeck coefficients can vary by as much as 8 μV/K for any given sample). In theory, the less a p-type semiconductor is doped the lower the Seebeck coefficient value should be. Since the amount of Ca is roughly the same throughout each sample it's hard to gain a reasonable conclusion. It seems as though the fluence used when creating each sample did to some extent determine the amount of calcium in the sample (the lowest, sample 110223, at 1.0 J/m^2 only had 1.79% Ca while samples 110222 (2.38% Ca) and 110223-03 (2.37% Ca) were made with the highest fluence, 1.5 and 1.75 respectively (Appendix C), but that it bore no real connection to the Seebeck coefficients obtained. Taking a look at the Bi:O and Cu:Se ratios (Appendix C) some insight into the impurities of the samples are seen. These samples are not perfect BiCuOSe:Ca samples and thus may not behave as we may theorize they should.

Using the Chaikin and Beni model to compare the carrier concentration to the Hall carrier concentration of the front side of the ITO sample (Table 3.1) we see that in all three Chaikin and Beni models that the model is higher by an order of magnitude than that of the Hall carrier concentration, however the amount that the model is off seems to decrease as we account for the nearest neighbor interaction. It may be that if we accounted for the next neighboring interaction (j = 2) that the model would be a little more agreeable to the Hall model. The same is true to an extent for the back side of the ITO sample, however the back seems to disagree a whole lot more than does the front, the Chaikin and Beni model is at least 2 orders of magnitude larger than the Hall model. It does seem to decrease a little as the next nearest neighbor interaction is taken into account, but it does not seem to decrease dramatically. This could mean that not enough neighbors are being accounted for, but it could also mean that 300 K is not a high enough

temperature limit for Chaikin and Beni's proposed theory for ITO.

ITO Front

	Region where $kT>>U_0, U_j$		Region where $U_0 >>kT>> U_j, T$		Region where $U_0 >U_1>kT>> U_{j>1}, T$		
Temp. (K)	Hall ρ (cm^{-3})	Chaikin and Beni ρ (cm^{-3})	Hall ρ (cm^{-3})	Chaikin and Beni ρ (cm^{-3})	Hall ρ (cm^{-3})	Chaikin and Beni ρ (cm^{-3})	
						ρ_1	ρ_2
18	7.84E+20	5.15E+21	7.84E+20	7.71E+21	7.84E+20	2.58E+21	5.19E+21
40	7.69E+20	5.13E+21	7.69E+20	7.65E+21	7.69E+20	2.57E+21	5.19E+21
60	7.81E+20	5.11E+21	7.81E+20	7.61E+21	7.81E+20	2.56E+21	5.20E+21
80	7.85E+20	5.09E+21	7.85E+20	7.58E+21	7.85E+20	2.56E+21	5.20E+21
100	7.90E+20	5.08E+21	7.90E+20	7.55E+21	7.90E+20	2.56E+21	5.21E+21
120	7.89E+20	5.07E+21	7.89E+20	7.53E+21	7.89E+20	2.55E+21	5.21E+21
140	7.89E+20	5.05E+21	7.89E+20	7.48E+21	7.89E+20	2.55E+21	5.22E+21
160	7.94E+20	5.05E+21	7.94E+20	7.48E+21	7.94E+20	2.54E+21	5.22E+21
180	7.93E+20	5.03E+21	7.93E+20	7.44E+21	7.93E+20	2.54E+21	5.23E+21
200	7.89E+20	5.02E+21	7.89E+20	7.41E+21	7.89E+20	2.53E+21	5.23E+21
220	7.93E+20	5.00E+21	7.93E+20	7.38E+21	7.93E+20	2.53E+21	5.23E+21
239	7.98E+20	4.99E+21	7.98E+20	7.36E+21	7.98E+20	2.53E+21	5.24E+21
259	7.81E+20	4.98E+21	7.81E+20	7.34E+21	7.81E+20	2.52E+21	5.24E+21
278	7.81E+20	4.96E+21	7.81E+20	7.28E+21	7.81E+20	2.51E+21	5.25E+21
298	7.86E+20	4.97E+21	7.86E+20	7.31E+21	7.86E+20	2.52E+21	5.25E+21

ITO Back

	Region where $kT>>U_0, U_j$		Region where $U_0 >>kT>> U_j, T$		Region where $U_0 >U_1>kT>> U_{j>1}, T$		
Temp. (K)	Hall ρ (cm^{-3})	Chaikin and Beni ρ (cm^{-3})	Hall ρ (cm^{-3})	Chaikin and Beni ρ (cm^{-3})	Hall ρ (cm^{-3})	Chaikin and Beni ρ (cm^{-3})	
						ρ_1	ρ_2
22	1.27E+19	5.12E+21	1.27E+19	7.65E+21	1.27E+19	2.57E+21	5.19E+21
33	1.33E+19	5.10E+21	1.33E+19	7.59E+21	1.33E+19	2.56E+21	5.20E+21
44	1.32E+19	5.07E+21	1.32E+19	7.54E+21	1.32E+19	2.55E+21	5.21E+21
66	1.31E+19	5.02E+21	1.31E+19	7.43E+21	1.31E+19	2.54E+21	5.23E+21
77	1.39E+19	4.98E+21	1.39E+19	7.34E+21	1.39E+19	2.52E+21	5.24E+21
88	1.36E+19	4.96E+21	1.36E+19	7.30E+21	1.36E+19	2.52E+21	5.25E+21
110	1.40E+19	4.95E+21	1.40E+19	7.26E+21	1.40E+19	2.51E+21	5.25E+21
132	1.43E+19	4.87E+21	1.43E+19	7.09E+21	1.43E+19	2.49E+21	5.28E+21
154	1.37E+19	4.83E+21	1.37E+19	7.01E+21	1.37E+19	2.47E+21	5.29E+21
176	1.42E+19	4.79E+21	1.42E+19	6.93E+21	1.42E+19	2.46E+21	5.31E+21
198	1.45E+19	4.75E+21	1.45E+19	6.85E+21	1.45E+19	2.45E+21	5.32E+21
220	1.46E+19	4.72E+21	1.46E+19	6.78E+21	1.46E+19	2.44E+21	5.33E+21
242	1.51E+19	4.68E+21	1.51E+19	6.70E+21	1.51E+19	2.42E+21	5.34E+21
263.5	1.45E+19	4.66E+21	1.45E+19	6.66E+21	1.45E+19	2.42E+21	5.35E+21
286	1.45E+19	4.59E+21	1.45E+19	6.52E+21	1.45E+19	2.39E+21	5.37E+21

BiCuOSe:Ca

		Region where $kT>>U_0, U_j$		Region where $U_0 >>kT>> U_j, T$		Region where $U_0 >U_1>kT>> U_{j>1}, T$		
Sample #	Temp. (K)	Hall ρ (cm^{-3})	Chaikin and Beni ρ (cm^{-3})	Hall ρ (cm^{-3})	Chaikin and Beni ρ (cm^{-3})	Hall ρ (cm^{-3})	Chaikin and Beni ρ (cm^{-3})	
							ρ_1	ρ_2
110222	300	5.48E+20	1.12E+22	5.48E+20	1.10E+22	5.48E+20	4.27E+21	1.03E+22
110223	300	5.61E+20	1.09E+22	5.61E+20	1.18E+22	5.61E+20	4.42E+21	1.02E+22
110223-0	300	5.77E+20	1.13E+22	5.77E+20	1.08E+22	5.77E+20	4.24E+21	1.04E+22
110224	300	6.43E+20	1.09E+22	6.43E+20	1.17E+22	6.43E+20	4.40E+21	1.02E+22

Table 3.1: *The Hall carrier concentration and the Chaikin and Beni carrier concentration seem to differ by at least and order of magnitude for temperatures between 22 -300 K. This probably indicates that 300 K is not a high enough temperature limit for the Chaikin and Beni model.*

When the Chaikin and Beni model is applied to the four samples of BiCuOSe:Ca we see that the same type of pattern is present (see Table 3.1). That is, the Chaikin and Beni model disagrees with the Hall model by two orders of magnitude. The Hall carrier concentration (in cm^{-3}) is around 10^{20} cm^{-3} while the Chaikin and Beni model suggests a carrier concentration of about 10^{22} cm^{-3}. The Chaikin and Beni carrier concentration tends to decrease slightly with the number of neighboring interactions, but not by much. I believe that 300 K is most likely not a high enough temperature limit for which the Chaikin and Beni model applies.

By assuming that both of the models were linear with temperature I solved for the temperature at which both of the models would be in agreement (for the ITO data), that is, the high temperature limit. The ITO front data set the high temperature limit at 5753 K for the region where $kT>>U_0, U_j,$ 6990 K for the region where $U_0 >>kT>> U_j, T,$ and 9565 K for the region where $U_0 >U_1>kT>> U_{j>1}, T.$ The ITO back data set the high temperature limit at 3981 K for the region where $kT>>U_0, U_j,$ 1994 K for the region where $U_0 >>kT>> U_j, T$, and 4229 K for the region where $U_0 >U_1>kT>> U_{j>1}, T$. The region where $U_0 >U_1>kT>> U_{j>1}, T$ yields two roots for the Chaikin and Beni carrier concentration (as the Seebeck coefficient is a quadratic function), using the lower of the two roots (ρ_1) allows a high temperature limit to be found while the higher root (ρ_2) will return an invalid temperature (negative K). Easley, 2003 explores the Chaikin and Beni theory further.

Section 4: Conclusions

In conclusion, the Seebeck coefficients for BiCuOSe:Ca doped at 1.79%, 2.38%, 2.37%, and 2.27% (Appendix C) all to behave metallically with decreasing temperature. Since the amount of doping does not differ by much between these samples, no real correlation between the amount of calcium present and the Seebeck coefficient can be made. It is clear, however, that all of the samples, regardless of how much calcium was present in them, exhibit this metallic trend which is consistent with previous BiCuOSe:Ca results reported in Zakutayev, 2011. Although the Seebeck coefficients themselves of this experiment were much lower (at room temperature) than that of undoped BiCuOSe and the 10% doped BiCuOSe:Ca obtained by them (150 μV/K and 130 μV/K respectively for their undoped and 10% sample compared to this experiment's results of 43.908 μV/K (2.38%), 33.1 μV/K (1.79%), 45.9 μV/K (2.37%), and 34.7 μV/K (2.27%)). Typically the Seebeck coefficient decreases with increased doping, but for these samples that pattern is not seen. The ratios of Bi:O and Cu:Se give insight into the impurities of the samples which may account for

The method by Chaikin and Beni to determine the carrier concentration from the Seebeck coefficient and resistivity at a high temperature limit of 300 K for ITO on both the front and back of the sample yielded a carrier concentration that was at least an order of magnitude greater than what was determined by the Hall measurements. The degree at which the Chaikin and Beni model differed from the Hall model seemed to decrease slightly when nearest neighbor interactions were taken into account, but it seems as though 300 K is not a high enough temperature limit for which to apply Chaikin and Beni model

Likewise, for the samples of BiCuOSe:Ca measured in this experiment, the Chaikin and Beni model is about two orders of magnitude greater than the Hall model . As the next nearest neighbor interaction is taken into account the extent at which the Chaikin and Beni model and the Hall model seems to decrease slightly. Perhaps with more neighboring atom interactions the models would agree better, but it is my belief that the significant difference in the Chaikin and Beni model and the Hall model is because 300 K is not a high enough temperature limit for the Chaikin and Beni model. Through iteration I determined that the high temperature limit for which to apply the Chaikin and Beni model (the limit where the Chaikin and Beni model matches that of the Hall) is between 2000-10,000 K.

Appendix A: Carrier Concentration of Chaikin and Beni for ITO and BiCuOSe:Ca

ITO Front

ITO FRONT

volume (angstrom)	1.03E+03
volume (cm^{-3})	1.03E-21
carrier hosts in cell	8
sites per unit vol. (cm^{-3})	7.76E+21
e (Coulomb)	1.60E-19
boltzman const. (eV/K)	8.62E-05
k/e	8.62E-05

*carrier concentration measured in cm^-3

Region where the on-site coulomb interaction is much greater than kT which is greater than the coulomb interaction between sites j units apart (U_j)

Hall ρ (cm^{-3})	Chaikin and Beni ρ (cm^{-3})	Temp. (K)	Seebeck (μV/K)	Resistivity (Ωcm)	(1-c)/c	C = fraction of holes
7.84E+20	5.15E+21	18	-1.30E+00	N/a	5.08E-01	6.63E-01
7.69E+20	5.13E+21	40	-2.50E+00	2.25E-04	5.15E-01	6.60E-01
7.81E+20	5.11E+21	60	-3.50E+00	2.25E-04	5.21E-01	6.58E-01
7.85E+20	5.09E+21	80	-4.20E+00	2.25E-04	5.25E-01	6.56E-01
7.90E+20	5.08E+21	100	-4.70E+00	2.26E-04	5.28E-01	6.54E-01
7.89E+20	5.07E+21	120	-5.20E+00	2.26E-04	5.31E-01	6.53E-01
7.89E+20	5.05E+21	140	-6.30E+00	2.28E-04	5.38E-01	6.50E-01
7.94E+20	5.05E+21	160	-6.40E+00	2.31E-04	5.39E-01	6.50E-01
7.93E+20	5.03E+21	180	-7.30E+00	2.33E-04	5.44E-01	6.48E-01
7.89E+20	5.02E+21	200	-7.90E+00	2.36E-04	5.48E-01	6.46E-01
7.93E+20	5.00E+21	220	-8.50E+00	2.37E-04	5.52E-01	6.44E-01
7.98E+20	4.99E+21	239	-9.10E+00	2.40E-04	5.56E-01	6.43E-01
7.81E+20	4.98E+21	259	-9.40E+00	2.43E-04	5.58E-01	6.42E-01
7.81E+20	4.96E+21	278	-1.08E+01	2.46E-04	5.67E-01	6.38E-01
7.86E+20	4.97E+21	298	-1.01E+01	N/A	5.62E-01	6.40E-01

Region where kT is much bigger than the on-site coulomb interaction and U_i

Hall ρ (cm^{-3})	Chalkin and Beni ρ (cm^{-3})	Temp. (K)	Seebeck (μV/K)	Resistivity (Ωcm)	(2-c)/c	C = fraction of holes
7.84E+20	7.71E+21	18	-1.30E+00	N/a	1.02E+00	9.92E-01
7.69E+20	7.65E+21	40	-2.50E+00	2.25E-04	1.03E+00	9.85E-01
7.81E+20	7.61E+21	60	-3.50E+00	2.25E-04	1.04E+00	9.80E-01
7.85E+20	7.58E+21	80	-4.20E+00	2.25E-04	1.05E+00	9.76E-01
7.90E+20	7.55E+21	100	-4.70E+00	2.26E-04	1.06E+00	9.73E-01
7.89E+20	7.53E+21	120	-5.20E+00	2.26E-04	1.06E+00	9.70E-01
7.89E+20	7.48E+21	140	-6.30E+00	2.28E-04	1.08E+00	9.63E-01
7.94E+20	7.48E+21	160	-6.40E+00	2.31E-04	1.08E+00	9.63E-01
7.93E+20	7.44E+21	180	-7.30E+00	2.33E-04	1.09E+00	9.58E-01
7.89E+20	7.41E+21	200	-7.90E+00	2.36E-04	1.10E+00	9.54E-01
7.93E+20	7.38E+21	220	-8.50E+00	2.37E-04	1.10E+00	9.51E-01
7.98E+20	7.36E+21	239	-9.10E+00	2.40E-04	1.11E+00	9.47E-01
7.81E+20	7.34E+21	259	-9.40E+00	2.43E-04	1.12E+00	9.46E-01
7.81E+20	7.28E+21	278	-1.08E+01	2.46E-04	1.13E+00	9.37E-01
7.86E+20	7.31E+21	298	-1.01E+01	N/A	1.12E+00	9.41E-01

Region where the on-site coulomb interaction is greater than the nearest neighbor interaction which is much greater than kT which is much greater than the high temp limit and U_i

Hall ρ (cm^{-3})	Chalkin and Beni ρ (cm^{-3})		Temp. (K)	Seebeck (μV/K)	Resistivity (Ωcm)	$2(1-2c)^2/c(1-c)$	C = fraction of holes	
	ρ_1	ρ_2				c_1		c_2
7.84E+20	2.58E+21	5.19E+21	18	-1.30E+00	N/a	5.08E-01	3.32E-01	6.68E-01
7.69E+20	2.57E+21	5.19E+21	40	-2.50E+00	2.25E-04	5.15E-01	3.31E-01	6.69E-01
7.81E+20	2.56E+21	5.20E+21	60	-3.50E+00	2.25E-04	5.21E-01	3.30E-01	6.70E-01
7.85E+20	2.56E+21	5.20E+21	80	-4.20E+00	2.25E-04	5.25E-01	3.30E-01	6.70E-01
7.90E+20	2.56E+21	5.21E+21	100	-4.70E+00	2.26E-04	5.28E-01	3.29E-01	6.71E-01
7.89E+20	2.55E+21	5.21E+21	120	-5.20E+00	2.26E-04	5.31E-01	3.29E-01	6.71E-01
7.89E+20	2.55E+21	5.22E+21	140	-6.30E+00	2.28E-04	5.38E-01	3.28E-01	6.72E-01
7.94E+20	2.54E+21	5.22E+21	160	-6.40E+00	2.31E-04	5.39E-01	3.28E-01	6.72E-01
7.93E+20	2.54E+21	5.23E+21	180	-7.30E+00	2.33E-04	5.44E-01	3.27E-01	6.73E-01
7.89E+20	2.53E+21	5.23E+21	200	-7.90E+00	2.36E-04	5.48E-01	3.26E-01	6.74E-01
7.93E+20	2.53E+21	5.23E+21	220	-8.50E+00	2.37E-04	5.52E-01	3.26E-01	6.74E-01
7.98E+20	2.53E+21	5.24E+21	239	-9.10E+00	2.40E-04	5.56E-01	3.25E-01	6.75E-01
7.81E+20	2.52E+21	5.24E+21	259	-9.40E+00	2.43E-04	5.58E-01	3.25E-01	6.75E-01
7.81E+20	2.51E+21	5.25E+21	278	-1.08E+01	2.46E-04	5.67E-01	3.24E-01	6.76E-01
7.86E+20	2.52E+21	5.25E+21	298	-1.01E+01	N/A	5.62E-01	3.24E-01	6.76E-01

ITO Back

ITO BACK

volume (angstrom)	1.03E+03	
volume (cm^{-3})	1.03E-21	*carrier concentration measured in cm^-3
carrier hosts in cell	8	
sites per unit vol. (cm^{-3})	7.76E+21	
e (Coulomb)	1.60E-19	
boltzman const. (eV/K)	8.62E-05	
k/e	8.62E-05	

Region where the on-site coulomb interaction is much greater than kT which is greater than the coulomb interaction between sites j units apart (U_j)

Hall ρ (cm^{-3})	Chalkin and Beni ρ (cm^{-3})	Temp. (K)	Seebeck (μV/K)	Resistivity (Ωcm)	(1-c)/c	C = fraction of holes
1.27E+19	5.12E+21	22	-2.60E+00	2.74E-02	5.15E-01	6.60E-01
1.33E+19	5.10E+21	33	-3.90E+00	2.72E-02	5.23E-01	6.57E-01
1.32E+19	5.07E+21	44	-5.10E+00	2.71E-02	5.30E-01	6.53E-01
1.31E+19	5.02E+21	66	-7.50E+00	2.69E-02	5.45E-01	6.47E-01
1.39E+19	4.98E+21	77	-9.40E+00	2.66E-02	5.58E-01	6.42E-01
1.36E+19	4.96E+21	88	-1.04E+01	2.66E-02	5.64E-01	6.39E-01
1.40E+19	4.95E+21	110	-1.13E+01	2.62E-02	5.70E-01	6.37E-01
1.43E+19	4.87E+21	132	-1.50E+01	2.58E-02	5.95E-01	6.27E-01
1.37E+19	4.83E+21	154	-1.69E+01	2.56E-02	6.08E-01	6.22E-01
1.42E+19	4.79E+21	176	-1.87E+01	2.56E-02	6.21E-01	6.17E-01
1.45E+19	4.75E+21	198	-2.05E+01	2.57E-02	6.34E-01	6.12E-01
1.46E+19	4.72E+21	220	-2.19E+01	2.58E-02	6.45E-01	6.08E-01
1.51E+19	4.68E+21	242	-2.37E+01	2.59E-02	6.58E-01	6.03E-01
1.45E+19	4.66E+21	263.5	-2.47E+01	2.60E-02	6.66E-01	6.00E-01
1.45E+19	4.59E+21	286	-2.78E+01	2.58E-02	6.90E-01	5.92E-01

Region where kT is much bigger than the on-site coulomb interaction and U_i

Hall ρ (cm^{-3})	Chalkin and Beni ρ (cm^{-3})	Temp. (K)	Seebeck (μV/K)	Resistivity (Ωcm)	(2-c)/c	C = fraction of holes
1.27E+19	7.65E+21	22	-2.60E+00	2.74E-02	1.03E+00	9.85E-01
1.33E+19	7.59E+21	33	-3.90E+00	2.72E-02	1.05E+00	9.77E-01
1.32E+19	7.54E+21	44	-5.10E+00	2.71E-02	1.06E+00	9.70E-01
1.31E+19	7.43E+21	66	-7.50E+00	2.69E-02	1.09E+00	9.57E-01
1.39E+19	7.34E+21	77	-9.40E+00	2.66E-02	1.12E+00	9.46E-01
1.36E+19	7.30E+21	88	-1.04E+01	2.66E-02	1.13E+00	9.40E-01
1.40E+19	7.26E+21	110	-1.13E+01	2.62E-02	1.14E+00	9.35E-01
1.43E+19	7.09E+21	132	-1.50E+01	2.58E-02	1.19E+00	9.13E-01
1.37E+19	7.01E+21	154	-1.69E+01	2.56E-02	1.22E+00	9.02E-01
1.42E+19	6.93E+21	176	-1.87E+01	2.56E-02	1.24E+00	8.92E-01
1.45E+19	6.85E+21	198	-2.05E+01	2.57E-02	1.27E+00	8.82E-01
1.46E+19	6.78E+21	220	-2.19E+01	2.58E-02	1.29E+00	8.74E-01
1.51E+19	6.70E+21	242	-2.37E+01	2.59E-02	1.32E+00	8.63E-01
1.45E+19	6.66E+21	263.5	-2.47E+01	2.60E-02	1.33E+00	8.58E-01
1.45E+19	6.52E+21	286	-2.78E+01	2.58E-02	1.38E+00	8.40E-01

Region where the on-site coulomb interaction is greater than the nearest neighbor interaction which is much greater than kT which is much greater than the high temp limit and U_i

Hall ρ (cm^{-3})	Chalkin and Beni ρ (cm^{-3})		Temp. (K)	Seebeck (μV/K)	Resistivity (Ωcm)	$2(1-2c)^2/c(1-c)$	C = fraction of holes		
	ρ_1	ρ_2					c_1	c_2	
1.27E+19	2.57E+21	5.19E+21	22	-2.60E+00	2.74E-02	5.15E-01	3.31E-01	6.69E-01	
1.33E+19	2.56E+21	5.20E+21	33	-3.90E+00	2.72E-02	5.23E-01	3.30E-01	6.70E-01	
1.32E+19	2.55E+21	5.21E+21	44	-5.10E+00	2.71E-02	5.30E-01	3.29E-01	6.71E-01	
1.31E+19	2.54E+21	5.23E+21	66	-7.50E+00	2.69E-02	5.45E-01	3.27E-01	6.73E-01	
1.39E+19	2.52E+21	5.24E+21	77	-9.40E+00	2.66E-02	5.58E-01	3.25E-01	6.75E-01	
1.36E+19	2.52E+21	5.25E+21	88	-1.04E+01	2.66E-02	5.64E-01	3.24E-01	6.76E-01	
1.40E+19	2.51E+21	5.25E+21	110	-1.13E+01	2.62E-02	5.70E-01	3.23E-01	6.77E-01	
1.43E+19	2.49E+21	5.28E+21	132	-1.50E+01	2.58E-02	5.95E-01	3.20E-01	6.80E-01	
1.37E+19	2.47E+21	5.29E+21	154	-1.69E+01	2.56E-02	6.08E-01	3.18E-01	6.82E-01	
1.42E+19	2.46E+21	5.31E+21	176	-1.87E+01	2.56E-02	6.21E-01	3.17E-01	6.83E-01	
1.45E+19	2.45E+21	5.32E+21	198	-2.05E+01	2.57E-02	6.34E-01	3.15E-01	6.85E-01	
1.46E+19	2.44E+21	5.33E+21	220	-2.19E+01	2.58E-02	6.45E-01	3.14E-01	6.86E-01	
1.51E+19	2.42E+21	5.34E+21	242	-2.37E+01	2.59E-02	6.58E-01	3.12E-01	6.88E-01	
1.45E+19	2.42E+21	5.35E+21	263.5	-2.47E+01	2.60E-02	6.66E-01	3.11E-01	6.89E-01	
1.45E+19	2.39E+21	5.37E+21	286	-2.78E+01	2.58E-02	6.90E-01	3.08E-01	6.92E-01	

BiCuOSe:Ca

BiCuOSe

volume (angstrom)	1.37E+02	
volume (cm^{-3})	1.37E-22	*carrier concentration measured in cm^-3
carrier hosts in cell	2	
sites per unit vol. (cm^{-3})	1.46E+22	
e (Coulomb)	1.60E-19	
boltzman const. (eV/K)	8.62E-05	
k/e	8.62E-05	

Region where the on-site coulomb interaction is much greater than kT which is greater than the coulomb interaction between sites j units apart U_j)

Sample #	% Doped	Hall ρ (cm^{-3})	Chalkin and Beni ρ (cm^{-3})	Temp. (K)	Seebeck (μV/K)	Resistivity (Ωcm)	(1-c)/c	C = fraction of holes
110222	2.38%	5.48E+20	1.12E+22	300	4.39E+01	4.06E-03	3.00E-01	7.69E-01
110223	1.79%	5.61E+20	1.09E+22	300	3.31E+01	5.49E-03	3.41E-01	7.46E-01
110223-03	2.37%	5.77E+20	1.13E+22	300	4.59E+01	4.40E-03	2.94E-01	7.73E-01
110224	2.27%	6.43E+20	1.09E+22	300	3.47E+01	3.67E-03	3.34E-01	7.50E-01

Region where kT is much bigger than the on-site coulomb interaction and U_j

Sample #	% Doped	Hall ρ (cm^{-3})	Chalkin and Beni ρ (cm^{-3})	Temp. (K)	Seebeck (μV/K)	Resistivity (Ωcm)	(1-c)/c	C = fraction of holes
110222	2.38%	5.48E+20	1.10E+22	300	4.39E+01	4.06E-03	1.66E+00	7.51E-01
110223	1.79%	5.61E+20	1.18E+22	300	3.31E+01	5.49E-03	1.47E+00	8.10E-01
110223-03	2.37%	5.77E+20	1.08E+22	300	4.59E+01	4.40E-03	1.70E+00	7.40E-01
110224	2.27%	6.43E+20	1.17E+22	300	3.47E+01	3.67E-03	1.50E+00	8.01E-01

Region where the on-site coulomb interaction is greater than the nearest neighbor interaction which is much greater than kT which is much greater than the high temp limit and U_j

Sample #	% Doped	Hall ρ (cm^{-3})	Chalkin and Beni ρ (cm^{-3})		Temp. (K)	Seebeck (μV/K)	Resistivity (Ωcm)	(1-c)/c	C = fraction of holes	
			ρ_1	ρ_2					c_1	c_2
110222	2.38%	5.48E+20	4.27E+21	1.03E+22	300	4.39E+01	4.06E-03	8.32E-01	2.92E-01	7.08E-01
110223	1.79%	5.61E+20	4.42E+21	1.02E+22	300	3.31E+01	5.49E-03	7.34E-01	3.03E-01	6.97E-01
110223-03	2.37%	5.77E+20	4.24E+21	1.04E+22	300	4.59E+01	4.40E-03	8.52E-01	2.91E-01	7.09E-01
110224	2.27%	6.43E+20	4.40E+21	1.02E+22	300	3.47E+01	3.67E-03	7.48E-01	3.02E-01	6.98E-01

Appendix B: Lattice Parameters of BiCuOSe

The following outlines the lattice parameters and sites of BiCuOSe (courtesy of Prof. Janet Tate, Department of Physics, Oregon State University).

```
COL  ICSD Collection Code 75128
 DATE Recorded Oct 17, 1995
 NAME Bismuth copper(I) oxide selenide
 FORM Bi Cu O Se
      = Bi Cu O Se
 TITL New layered compounds with the general composition (MO) (CuSe),
      where M=Bi,Nd,Gd,Dy and BiOCuS: syntheses and crystal structure
 REF  Journal of Solid State Chemistry
      JSSCB 112 (1994) 189-191
 AUT  Kusainova A M, BerdonosovÿPÿS, AkselrudÿLÿG, KholodkovskayaÿLÿN,
      DolgikhÿVÿA, PopovkinÿBÿA
 CELL a=3.921(0) b=3.921(0) c=8.913(1) à=90.0 á=90.0 ç=90.0
      V=137.1 Z=2
 SGR  P 4/n m m Z   (129) - tetragonal
 CLAS 4/mmm (Hermann-Mauguin) - D4h (Schoenflies)
 PRS  tP8
 ANX  ABXY
 PARM Atom__No OxStat  Wyck -----X----- -----Y----- -----Z-----  -SOF-
      Bi     1  3.000    2c  1/4         1/4         0.1411(7)
      Se     1 -2.000    2c  1/4         1/4         0.680(2)
      Cu     1  1.000    2b  3/4         1/4         1/2
      O      1 -2.000    2a  3/4         1/4         0.
 WYCK c2 b a
 ITF  Bi  1   B=1.080(3)
 ITF  Se  1   B=1.360(9)
 ITF  Cu  1   B=2.600(2)
 ITF  O   1   B=0.307(4)
 REM  TEM 298
 REM  XDP (X-ray diffraction from a powder)
 REM  RVP
 RVAL 0.053
```

Appendix C: Hall Parameters and BiCuOSe:Ca Sample Composition

Hall Data and Composition courtesy of Jason Francis, Department of Physics (graduate student), Oregon State University.

Hall Measurements

Sample	Fluence (J/Cm^2)	Mobility (cm^2/(Vs))	Resistivity (Ωcm)	Carrier Concentration (cm^{-3})
110222	1.5	2.8094	4.06E-03	5.48E+20
110223	1	2.0243	5.49E-03	5.61E+20
110223-03	1.75	2.4552	4.40E-03	5.77E+20
110224	1.25	2.6949	3.67E-03	6.43E+20

EPMA

Sample	Ca	Bi	Cu	O	Se	Total	Ratio Bi:O	Ratio Cu:Se
110222	0.0238	0.1982	0.375	0.1515	0.2514	0.9999	1.31E+00	1.49E+00
110223	0.0179	0.1726	0.2744	0.3346	0.2005	1	5.16E-01	1.37E+00
110223-03	0.0237	0.2366	0.3698	0.0959	0.274	1	2.47E+00	1.35E+00
110224	0.0227	0.2463	0.4016	0.0461	0.2834	1.0001	5.34E+00	1.42E+00

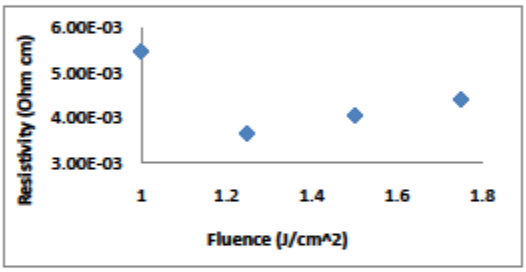

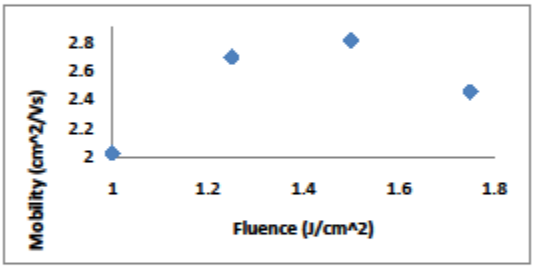

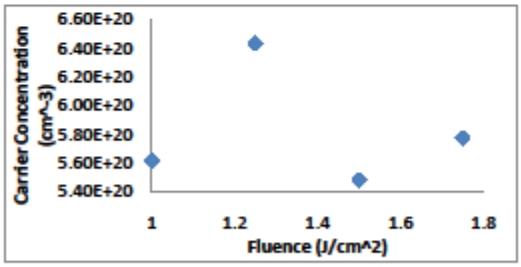

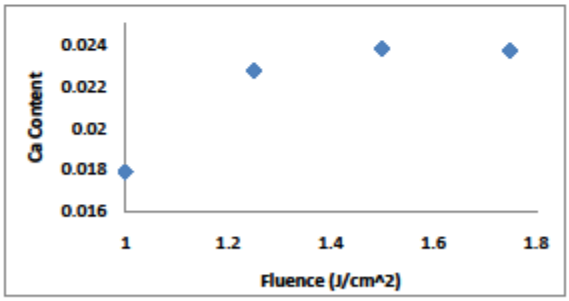

Bibliography

Chaikin, P. M., and G. Beni. "Thermopower in the correlated hopping regime." *Physical Review B* 13, no. 2 (January 1976): 647-651.

Easley, Dara. "Room Temperature Seebeck Measurements on $CuSc_{1-x}Mg_xO_{2+y}$ Transparent Conductive Thin Films." Oregon State University Department of Physics, February 7, 2003.

Gonzalez, Gabriela B., Jerome B. Cohen, Jin-Ha Hwang, Thomas O. Mason, Jason P. Hodges, and James D. Jorgensen. "Neutron diffraction study on the defect structure of indium-tin-oxide." *Journal of Applied Physics* 89, no. 5 (March 2001): 2550-2555.

Kasap, S. *Thermoelectric Effects in Metals: Thermocouples.* 1996. Http://Materials.Usask.Ca (accessed 3 2011, April).

MatWeb Material Property Data. *Hoskins Manufacturing Chromel® Thermocouple Wire Type K – Std.* 1996. http://www.matweb.com/search/datasheettext.aspx?matguid=26f6327db7f84c1e89e801461ae63851 (accessed April 23, 2011).

MatWeb Material Property Data. *Hoskins Manufacturing Alumel® Thermocouple Wire Type K – Std.* 1996. http://www.matweb.com/search/datasheettext.aspx?matguid=c8c0b158524a446bb953b781dee28efb (accessed April 23, 2011).

OMEGA Engineering. *Thermocouples- An Introduction.* 2003. http://www.omega.com/thermocouples.html (accessed February 4, 2011).

Seebeck, T. J. *Magnetische Polarisation der Metalle und Erzedurch Temperatur-Differenz.* Leipzig, Germany: Willhelm Engalmann, 1822.

Singh, Jasprit. *Semiconductor Devices: An Introduction.* McGraw-Hill, Inc., 1994.

Stampler, Evan S., William C. Sheets, Mariana I. Bertoni, Wilfrid Prellier, Thomas O. Mason, and Kenneth R. Poeppelmeier. "Temperature driven reactant solubilization synthesis of BiCuOSe." *Inorganic Chemistry* 47, no. 21 (July 2008): 10009-10016.

Tahar, R. B. H, T. Ban, Y. Ohya, and Y. Takahashi. "Tin doped indium oxide thin films: Electrical properties." *Journal of Applied Physics* 83, no. 5 (March 1998): 2631-2645.

Tan, Ming X., Paul E. Laibinis, Sonbinh T. Nguyen, Janet M. Kesselman, Colby E. Stanton, and Nathan S. Lewis. "Principles and Applications of Semiconductor Photoelectrochemistry." Edited by Kenneth D. Karlin. *Progress in Inorganic Chemistry* (John Wiley & Sons Inc.) 41 (1994).

Tate, Janet, et al. "Chalcogen-based transparent conductors." *Thin Solid Films* 516, no. 17 (July 2008): 5795-5799.

Zakutayev, A., P. F. Newhouse, Robert Kykyneshi, P. A. Hersh, D. A. Keszler, and J. Tate. "Pulsed laser deposition of BiCuOSe thin films." *Applied Physics A* 102, no. 2 (2011): 485-492.

Special Thanks To:

Prof. Janet Tate, Oregon State University, Department of Physics .

Prof. Brandon Brown, Department of Physics, University of San Francisco.

Dr. Robert Kykyneshi, Department of Chemistry, Oregon State University.

Jason Francis, Department of Physics (graduate student), Oregon State University.

Christopher Reidy, Department of Physics (graduate student), Oregon State University.